Point Mutations (Q19P and N23K) Increase the Operational Solubility of a 2α-*O*-Benzoyltransferase that Conveys Various Acyl Groups from CoA to a Taxane Acceptor

Irosha N. Nawarathne[†] and Kevin D. Walker*[,†,‡]

Department of Chemistry and Department of Biochemistry & Molecular Biology, Michigan State University, East Lansing, Michigan 48824

Received August 29, 2009

Two site-directed mutations within the wild-type 2-*O*-benzoyltransferase (*tbt*) cDNA, from *Taxus cuspidata* plants, yielded an encoded protein containing replacement amino acids at Q19P and N23K that map to a solvent-exposed loop region. The likely significant changes in the biophysical properties invoked by these mutations caused the overexpressed, modified TBT (*m*TBT) to partition into the soluble enzyme fraction about 5-fold greater than the wild-type enzyme. Sufficient protein could now be acquired to examine the scope of the substrate specificity of *m*TBT by incubation with 7,13-*O*,*O*-diacetyl-2-*O*-debenzoylbaccatin III that was mixed individually with various substituted benzoyls, alkanoyls, and (*E*)-butenoyl CoA donors. The *m*TBT catalyzed the conversion of each 7,13-*O*,*O*-diacetyl-2-*O*-debenzoylbaccatin III to several 7,13-*O*,*O*-diacetyl-2-*O*-acyl-2-*O*-debenzoylbaccatin III analogues. The relative catalytic efficiency of *m*TBT with the 7,13-*O*,*O*-diacetyl-2-*O*-debenzoyl surrogate substrate and heterole carbonyl CoA substrates was slightly greater than with the natural aroyl substrate benzoyl CoA, while substituted benzoyl CoA thioesters were less productive. Short-chain hydrocarbon carbonyl and cyclohexanoyl CoA thioesters were also productive, where C_4 substrates were transferred by *m*TBT with ~10- to 17-fold greater catalytic efficiency compared to the transfer of benzoyl. The described broad specificity of *m*TBT suggests that a plethora of 2-*O*-acyl variants of the antimitotic paclitaxel can be assembled through biocatalytic sequences.

Plant-derived acyltransferases that utilize a coenzyme A acyl donor and an amino or hydroxy group acceptor as cosubstrates are assigned to a large superfamily, designated BAHD.[1] These enzymes contain signature amino acid motifs such as an HXXXD, identified as catalytic (H) and structural (D) residues, and a DFGWG motif, located near the carboxyl terminus and presumed to comprise a substrate access channel. Occurrences of the BAHD acyltransferases are seemingly ubiquitous within the plant kingdom, and despite their prevalence, the function of several of the acyltransferases remain unknown. Of those that have been functionally characterized, very few have been extensively analyzed in terms of their substrate specificity profile. Generally, the BAHD catalysts principally acetylate and phenylpropanoylate amino and/or hydroxy groups of secondary metabolites.[2] In addition, benzoylation of plant secondary metabolites also occurs to invoke specific physiological effects in planta. The compendium of biosynthetic products made by these catalysts is a vast group of variously acylated metabolites found in different plant species.[1]

A cladogram of functionally characterized BAHD family members has been constructed on the basis of phylogenetic analysis of the protein sequences, and the evolutionary tree was shown to branch into five major clades.[1,3] All six of the benzoyltransferases in this superfamily reside in clade V, which includes *O*-benzoyltransferase (BEBT) isozymes from *Clarkia breweri* (AAN09796) and *Nicotiana tabacum* (AAN09798), a functionally similar benzyl/phenylethyl alcohol *O*-benzoyltransferase (BPBT, AAU06226) from *Petunia* × *hybrida*, the 2-*O*-debenzoylbaccatin III 2-*O*-benzoyltransferase (TBT, Q9FPW3) from *Taxus cuspidata* (described herein), and two *N*-acyltransferases, an *N*-debenzoylpaclitaxel *N*-benzoyltransferase (NDBTBT, AAM75818) from *Taxus canadensis*, and an anthranilate *N*-hydroxycinnamoyl/benzoyltransferase (HCBT, CAB06430) from *Dianthus caryophyllus*.[3] However, the substrate specificity of most recombinantly expressed and/or native BAHD benzoyltransferases (outside of the *Taxus* family) has been examined with only single or very limited substrates in standard steady-state kinetic evaluations in vitro.[1]

The application of the *O*-acyltransferases on the paclitaxel biosynthetic pathway toward the production of modified paclitaxel compounds can be greatly bolstered by knowledge of their substrate specificities with various taxane and acyl CoA thioester cosubstrates. To date, regarding biocatalytic *O*-acylation, the extended substrate specificity of only the paclitaxel pathway 10-*O*-acetyltransferase has been examined and was shown to be modest in its selectivity in vitro for three short-chain alkanoyl CoA's and to utilize 4- and 10-*O*-deacetyltaxanes, as acyl group acceptors.[4,5] Encouraged by the modest flexible specificity of the paclitaxel pathway *Taxus* *O*-acyltransferase examined thus far, an evaluation of the substrate selectivity of the 2-*O*-debenzoyltaxane 2-*O*-benzoyltransferase (TBT) with several substituted aroyl, alkanoyl, butenoyl, and heterole carbonyl CoA thioesters was performed. In a previous characterization of TBT, the transfer of benzoyl from the corresponding CoA thioesters to 7,13-*O*,*O*-diacetyl-2-*O*-debenzoylbaccatin III to form 7,13-*O*,*O*-diacetylbaccatin III was the primary focus, since 2-*O*-benzoylation is a necessary step in paclitaxel biosynthesis.[6] The substrate specificity was tested with only acetyl CoA, which was also found to be productive. Presented herein is a description of the expanded substrate specificity of a mutant TBT (*m*TBT) enzyme recombinantly expressed from *tbt* cDNA, which was altered by site-selected point mutations to fortuitously increase the solubility of the encoded protein over the wild-type form. The relative catalytic efficiency of *m*TBT with each productive substrate is reported, and the significance of utilizing the broad specificity of the paclitaxel pathway biocatalyst in the development of novel compounds is discussed.

Results and Discussion

Expression and Activity Assay of the 2-*O*-Benzoyltransferase. In a previous investigation,[6] the soluble wild-type TBT (wtTBT) enzyme was expressed from pCWori$^+$ in native form without an affinity tag.[7] The enzyme was partially purified by anion exchange chromatography and was characterized among other enzymes in a crude mixture containing 90 μg/mL of total protein.[6] The paucity of TBT expressed from the pCWori$^+$ vector without epitope tagging for selective purification prompted the exploration of a different expression system in the current study. The wild-type *tbt* cDNA was transferred from pCWori$^+$ into pET28a, and

* To whom correspondence should be addressed. Tel: 517 355-9715, ext 257. Fax: 517 353-1793. E-mail: walke284@msu.edu.
† Department of Chemistry.
‡ Department of Biochemistry & Molecular Biology.

10.1021/np900524d
Published on Web 01/28/2010

```
TBT_T. cuspidata_wt  : ------MGRFNVDMIERVIVAPCLQSPKNILHLSPIDNKT...
TBT_T. cuspidata_mut : ------MGRFNVDMIERVIVAPCLPSPKKILHLSPIDNKT...
TBT_T. media         : ------MGRFNVDMIERVIVAPCLPSPKKILRLSPIDNKT...
TBT_T. wallichiana   : ------MGRFNVDMIERVIVAPCLPSPKKILHLSPIDNKT...
DBAT_T. cuspidata    : MAGS---TEFVVRSLERVMVAPSQPSPKAFLQLSTLDNLP...
TAT_T. cuspidata     : MEKT----DLHVNLIEKVMVGPSPPLPKTTLQLSSIDNLP...
NDTBT_T. canadensis  : MEKAG-STDFHVKKFDPVMVAPSLPSPKATVQLSVVDSLT...
BPPT_T. cuspidata    : MKKTGSFAEFHVNMIERVMVRPCLPSPKTILPLSAIDNMA...
```

Figure 1. Partial amino acid sequence alignment of TBT (taxane 2α-*O*-benzoyltransferase) orthologues used to design the site-directed mutant of the wild-type TBT from *Taxus cuspidata*. The sequences of two TBT orthologues from *Taxus* × *media* and *T. wallichiana* and other operationally soluble *Taxus* acyltransferases involved in paclitaxel biosynthesis are included in the alignment. TBT_*T. cuspidata*_wt, wild-type TBT from *Taxus cuspidata* (accession no. AF297618); TBT_*T. cuspidata*_mut, site-directed mutant TBT with Q19P and N23K replacements; TBT_*T. media*, TBT from *Taxus* × *media* (accession no. AY675557); TBT_*T. wallichiana*, TBT from *Taxus wallichiana* (accession no. AY970522); DBAT_*T. cuspidata*, 10-deacetylbaccatin III 10-*O*-acetyltransferase from *Taxus cuspidata* (accession no. AF193765); TAT_*T. cuspidata*, taxadien-5α-ol *O*-acetyltransferase from *Taxus cuspidata* (accession no. AF190130); NDTBT_*T. canadensis*, 3′*N*-debenzoyl-2′-deoxytaxol *N*-benzoyltransferase from *Taxus canadensis* (accession no. AF466397); BPPT_*T. cuspidata*, 3-amino-3-phenylpropanoyltransferase from *Taxus cuspidata* (accession no. AY082804).

the resultant plasmid was designated p28wtTBT and was used to transform *Escherichia coli* BL21(DE3) cells. A significant portion (>95%) of wtTBT expressed in vivo as inactive inclusion bodies that partitioned with the insoluble fraction during initial attempts to solubly express the enzyme. wtTBT is probably functionally expressed at low concentration in the cells of its natural plant host, but when overexpressed in a heterologous host, it likely promoted the formation of a low-solubility aggregate.[8] This created a challenge to acquire sufficient wtTBT enzyme to complete the substrate specificity and kinetics analyses described herein. Several efforts were made, to no avail, to minimize or eliminate this challenge, including coexpression of the target cDNA with chaperone plasmids that encode proteins known to facilitate the folding process of expressed enzymes that tend to form inclusion bodies.[9] Numerous in vitro denaturing and refolding methodologies[10,11] were also attempted that either did not increase the fraction of functional soluble protein isolated as inclusion bodies from *E. coli* or did succeed at increasing the fraction of soluble protein, which was subsequently determined to be inactive.

Therefore, as an alternative to in vitro chemical manipulations to overcome the hydrophobic interactions that promote the formation of inclusion bodies, the sequence alignment of taxane 2-*O*-benzoyltransferase (TBT) orthologues was inspected more closely. General strategies for increasing protein solubility include site-directed mutagenesis, which aim to enhance solubility by replacing hydrophilic amino acids with others that contribute more favorably to interactions with bulk H_2O.[12] The sequence analysis revealed that TBT orthologues, isolated from *Taxus* × *media* and *T. wallichiana*, and other operationally soluble, functionally defined acyltransferases from *T. candensis* and *T. cuspidata* deposited in the GenBank database, contain a highly conserved proline (P) residue instead of a glutamine (Q) at position 19 of the wtTBT (Figure 1). Additionally, the two TBT orthologues contain tandem lysine residues (K22, K23). Guided by these parameters, the *tbt* cDNA obtained from *T. cuspidata* was mutated at codons CAA19CCA and AAT23AAA. Expression of the mutant *tbt* cDNA from the pET28a vector in *E. coli* yielded functional, recombinant mutant TBT (*m*TBT) protein (1 mg *m*TBT/L cells) containing two point-mutations (Q19P and N23K). This enzyme was fortuitously 5-fold more soluble than the identically expressed wild-type TBT (wtTBT) (200 μg of wtTBT/L cells), as determined by SDS-PAGE analysis and Coomassie blue staining (Figure 2) of the proteins in the respective soluble lysate from the *E. coli* cells. Western blot analysis of cell extracts from *E. coli* expressing p28wtTBT and p28PK-TBT further showed that the level of soluble *m*TBT was significantly increased over the expression of soluble wtTBT (Figure 3).

Furthermore, when the structure of wtTBT was modeled on the crystal structure of the related BAHD family vinorine synthase,

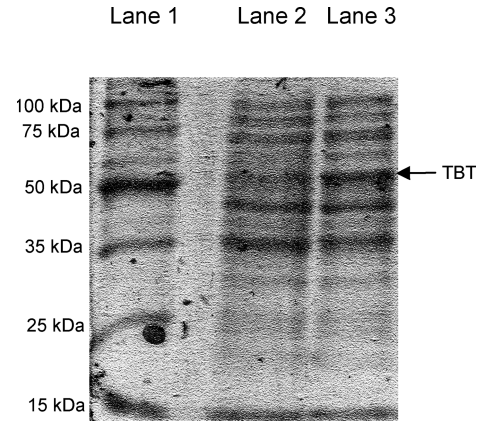

Figure 2. SDS polyacrylamide gel electrophoresis and Coomassie blue staining of recombinantly expressed, soluble wtTBT and *m*TBT (arrowed) isolated from *E. coli* BL21(DE3). Lane 1 contains molecular weight standards (Lonza); lane 2 shows the resolved proteins from 10 μg of total soluble protein from *E. coli* transformed with the p28wtTBT vector expressing the wild-type *tbt* cDNA insert; lane 3 shows the resolved proteins from 10 μg of total soluble protein from *E. coli* transformed with the p28PK-TBT vector expressing the CAA19CCA and AAT23AAA mutant *tbt* cDNA insert.

K23 was found to be part of a solvent-exposed loop structure positioned on the enzyme surface.[13,14] Since the internal pH of *E. coli* is approximated between 7.4 and 7.8,[15] the lysine side chain amino group (pK_a ~10) would also carry a partial net positive charge shared between the residues and would likely increase the protein solubility in bulk H_2O. In addition, the juxtaposition of K23 and K22 conceivably creates a dipole moment in the loop domain that could likely further facilitate soluble expression. This significant increase in soluble expression overcame the bottleneck to efficiently express TBT in operationally soluble form and therefore the production of functional catalyst was scaled-up to conduct the present substrate specificity investigation. Moreover, the mutant *tbt* cDNA was expressed with an *N*-terminal His_6-tag epitope for immunoblot verification and purification to ~70% purity by nickel-affinity resin chromatography. SDS-PAGE analysis of the partially purified *m*TBT revealed a dominant pair of proteins at R_f values consistent with those of chaperones GroEL and DnaK (57.4 and 69.1 kDa, respectively),[16] each comprising about 10% of the total protein (data not shown). The catalytic activity and quantity of *m*TBT in the presence of the presumed chaperones was judged sufficient for the purpose of the present investigation.

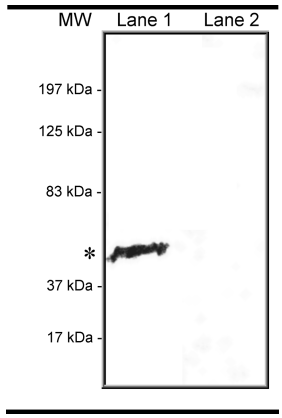

Figure 3. Western blot analysis of the soluble expression of wtTBT and *m*TBT enzyme in crude extracts of transformed *E. coli* cells. Comparison of the *m*TBT-His_6 fusion (lane 1) and the wtTBT-His_6 fusion (lane 2) by western-immunoblot analysis with the monoclonal anti-polyhistidine and anti-mouse IgG peroxidase conjugate. The band corresponding to the expressed *m*TBT protein is indicated by an asterisk. The locations of the molecular weight standards (Kaleidoscope Prestained Standards, Bio-Rad Laboratories) are shown.

Frequently, in vivo insolubility can result from low protein stability, where the hydrophobic sites normally buried within a protein can be exposed and interact with partially or completely unfolded protein in the expression host,[12] rendering the protein inactive. Therefore, protein solubility problems during overexpression might also be facilitated by approaches to increase protein stability. Proline is well known to define, in part, the conformation of secondary structural elements of proteins that provide structural rigidity, which often translates into structural stability when these pyrrolidine structures are situated proximally.[17] Proline residues are well conserved throughout the primary amino acid sequences (at 11 positions) of members of the BAHD acyltransferase superfamily involved in paclitaxel biosynthesis (see sequence alignment in the Supporting Information). The frequent occurrence of proline in the *Taxus* acyltransferases may contribute an important role in enzyme function and in defining the biophysical behavior of these catalysts. Although the inclusion of Q19P and N23K in *m*TBT represents modest mutations in terms of the primary amino acid sequence, these exchanges significantly influenced the physical properties that increased the soluble expression. Individual point mutants at each site were not constructed to separately dissect the effects of the individual mutations on the differential soluble expression of *m*TBT; this aspect will be probed in future investigations.

To initially screen for the function of the mutant 2-*O*-benzoyltransferase, [13-^{3}H]-7,13-*O*,*O*-diacetyl-2-*O*-debenzoylbaccatin III was synthesized on the basis of a combination of reported chemical transformations[18−20] (Scheme 1). The radiochemical material had the same retention time as authentic 7,13-*O*,*O*-diacetyl-2-*O*-debenzoylbaccatin III, synthesized from commercially available baccatin III, thus verifying the stereoselectivity of the borotritide reduction step (Scheme 1), and was consistent with findings in earlier studies.[21] The radiolabeled material was used in pilot-scale assays, similar to a previously described method,[6] and the appearance of a de novo biosynthetic product with similar retention time to that of authentic 7,13-*O*,*O*-diacetylbaccatin III prompted a large-scale assay to produce sufficient de novo biosynthetic product for characterization. *m*TBT (50 μg) was used in 1 mL assays with cosubstrate concentrations of the benzoyl CoA donor and taxane acceptor each at 1 mM. Direct injection on the LC-ESIMS confirmed the identity of the product as 7,13-*O*,*O*-diacetylbaccatin III, thus verifying that the mutant enzyme was functional.

Relative Substrate Specificity of *m*TBT with Various Aroyl CoA Thioesters and 7,13-*O*,*O*-Diacetyl-2-*O*-debenzoylbaccatin III. Pilot studies were initially conducted to determine the array of productive acyl CoA substrates from a small library of these activated thioesters that were synthesized by a previously described process[22] or obtained from commercial sources. After using radiolabeled 7,13-*O*,*O*-diacetyl-2-*O*-debenzoylbaccatin III and a single acyl CoA substrate in separate assays, 18 CoA thioesters, in addition to benzoyl CoA, were found to be utilized by *m*TBT. Each biosynthetic product was further characterized by incubating *m*TBT, 7,13-*O*,*O*-diacetyl-2-*O*-debenzoylbaccatin III at 1 mM, and the 2-*O*-benzoyltransferase separately with different acyl CoA substrates (1.0 mM). EtOAc was added to the assays to partition the acylated products into the organic phase. The extracted products were verified as 2-*O*-acyl taxane analogues by MS. The first-stage mass spectrometer was set to select for the $[M + H]^+$ ion of the product, which was directed into a fragmentation chamber, and the resulting fragment ions were analyzed by the second-stage mass spectrometer set to scan mode. Typical diagnostic fragment ions of 2-*O*-acyl-2-*O*-debenzoylbaccatin III analogues were evaluated using authentic 7,13-*O*,*O*-diacetylbaccatin III as a model to identify the various ion cleavage points. Diagnostic ions are *m*/*z* 671.2 $[M + H]^+$, 551.2 [*m*/*z* 671.2 − 2HOAc]$^+$, 491.2 [*m*/*z* 551 − HOAc]$^+$, 429.2 [*m*/*z* 551.2 − RCOOH at C-2]$^+$, 369.2 [*m*/*z* 429.2 − HOAc]$^+$, and 309.2 [*m*/*z* 369.2 − HOAc]$^+$. Analogous assays conducted with enzyme isolated from *E. coli* harboring the empty vector did not show detectable product derived from any of the acyl CoA's.

Most of the aroyl CoA's examined in this study were productive with *m*TBT and 7,13-*O*,*O*-diacetyl-2-*O*-debenzoylbaccatin III, when both substrates were assayed at 1 mM. The specificity constant (k_{cat}/K_M) of *m*TBT for each functional acyl CoA was estimated from the amount of the 2-*O*-acylated taxane made from the corresponding thioester in a competitive substrate reaction under typical assay conditions.[23] The compounds in the resulting product mixture were separated by reversed-phase HPLC with electrospray ionization of the effluent, and the abundance of the putative biosynthetic analyte ion was quantified by MS. When compared to the total number of ionizable heteroatoms in the entire biosynthetic molecules of, for example, 7,13-*O*,*O*-diacetyl-2-*O*-debenzoyl-2-*O*-(3-thiophenecarbonyl)baccatin III (molecular formula $C_{33}H_{40}O_{13}S$), the ionizable sites on the heterole side chains at the C-2 hydroxy group are about ∼8% (1-sulfur in the aryl side chain compared to 13-oxygen sites in the remainder of the molecule). Therefore, the mode of electrospray ionization of the 7,13-*O*,*O*-diacetylbaccatin III (the 2-*O*-benzoyl analogue) standard was deemed essentially similar to the ionization mechanism for each biosynthetic 2-*O*-acyl-2-*O*-debenzoyl analogue derived by *m*TBT catalysis, regardless of the C-2 side chain. Therefore, instead of synthesizing and characterizing the several different authentic standards corresponding to each proposed de novo 2-*O*-acyl biosynthetic product to calculate the concentrations of biosynthetic products, authentic 7,13-*O*,*O*-diacetylbaccatin III was used as the general standard for all of the 2-*O*-acyl analogues and quantitation of ion abundance by MS (see Supporting Information). Exemplary 7,13-*O*,*O*-diacetyl-2-*O*-acyl-2-*O*-debenzoylbaccatin III analogues were synthesized and analyzed identically by LC-ESIMS at concentrations similar to those of 7,13-*O*,*O*-diacetylbaccatin III. A correlation of 1:1 was observed between concentration and ion abundance among the 2-*O*-acyl analogues tested (data not shown), which supported the use of 7,13-*O*,*O*-diacetylbaccatin III as the all-purpose calibration standard.

Ion abundance was converted to analyte concentration by a linear regression equation that correlated the peak areas under the signals generated for selected ions $[M + H]^+$ and $[M + Na]^+$ detected by the mass spectrometer with a series of 7,13-*O*,*O*-diacetylbaccatin III standards at various concentrations. From the analysis of the ion abundances, the relative specificity constants (Table 1) were

Scheme 1. Synthesis of [13-^{3}H]-7,13-*O*,*O*-Diacetyl-2-*O*-debenzoylbaccatin III[a,b,c,d]

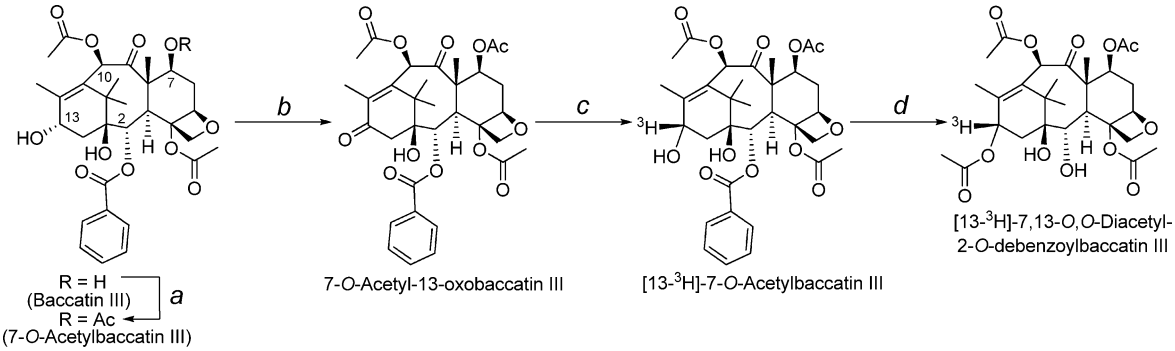

[a] Ac_2O, 4-DMAP, Et_3N, 97% yield.
[b] MnO_2, 100% yield.
[c] Sodium [^{3}H]borohydride, 0 °C, 0.61 mCi, 97% radiochemical purity.
[d] (i) Ac_2O, 4-DMAP, Et_3N, (ii) Red-Al, 0 °C, 0.35 mCi, 99% radiochemical purity.

Table 1. Relative Kinetics of *m*TBT with Aroyl- and Short-Chain Hydrocarbon-CoA's and 7,13-*O*,*O*-Diacetyl-2-*O*-debenzoylbaccatin III Co-substrates[a,b]

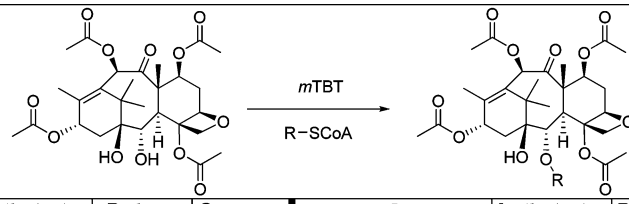

R Derived from CoA		A (k_{cat}/K_M) ($min^{-1}.mM^{-1}$)	B k_{cat} (min^{-1})	C K_M (μM)	R Derived from CoA		A (k_{cat}/K_M) ($min^{-1}.mM^{-1}$)	B k_{cat} (min^{-1})	C K_M (μM)
	**1**	1.8	0.19	110	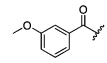	**13**	---	---	---
	**2**	---	---	---	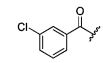	**14**	---	---	---
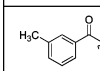	**3**	[b]---	[a]*2.4 × 10^{-3}*	---		**15**	0.38	0.016	42
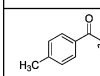	**4**	1.8	0.021	12		**16**	0.92	0.11	120
	**5**	3.9	0.65	170		**17**	2.2	0.014	6.4
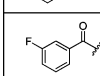	**6**	0.28	0.075	270		**18**	2.9	0.13	45
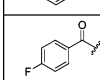	**7**	0.62	0.076	120		**19**	2.9	0.51	180
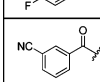	**8**	---	---	---		**20**	0.35	0.13	370
	**9**	0.49	0.25	510		**21**	---	---	---
	**10**	3.0	0.35	120		**22**	0.24	0.010	42
	**11**	21	1.2	57		**23**	0.42	0.023	55
	**12**	35	1.7	49		**24**	[b]---	[a]*2.6 × 10^{-4}*	---

[a] The rate of product formed by the transfer of the corresponding acyl group from CoA by *m*TBT catalysis was considered to be first-order (i.e., significantly below saturation); the value reported is v_o (nmol min^{-1}). [b] The catalytic efficiency was not calculated for these entries, since the corresponding acyl CoA's were not strong competitive inhibitors of benzoyl CoA in mixed substrate assays, and consequently, the associated products were not detectable. k_{cat}/K_M values are listed as min^{-1} mM^{-1}, k_{cat} values are listed as min^{-1}, and K_M values are listed as μM. The standard error for each of these parameters measured from triplicate assays is ~5%. The dashed line (---) indicates that the corresponding biosynthetic products were below the detection limits of the mass spectrometer.

calculated on the basis of the specificity constant (k_{cat}/K_M = 1.8 min^{-1} mM^{-1}) calculated for *m*TBT with benzoyl coenzyme A (entry 1A). The catalytic efficiency for 4-methylbenzoyl CoA (entry 4A) was equal to that of the natural substrate; the efficiency of *m*TBT for the other coenzyme A thioesters of substituted-aroyls or heterole carbonyls ranged from 0.28 to 3.9 min^{-1} mM^{-1} (Table 1, column A). The *p*-substituted aroyls within a homologous series had the highest catalytic efficiency, while the biosynthetic product in assays with the *m*- or *o*-substituted aroyl CoA's (Table 1, entries 2, 8, 13, and 14) was below the detection limits of the mass spectrometer. The *o*- and *m*-fluorobenzoyl CoA analogues and *m*-methylbenzoyl CoA were the exception; the catalytic efficiency with the *o*-fluoro substrate was 3.9 min^{-1} mM^{-1} (entry 5A) compared to 0.62 min^{-1} mM^{-1} for the *p*-fluoro isomer (entry 7A). While the *m*-methylbenzoyl CoA was productive, it was nevertheless transferred by *m*TBT at comparatively lower efficiency than the other productive acyl CoA's (entry 3). Intriguingly, *m*TBT showed higher catalytic efficiency with several of the acyclic and some heterocarbonyl thioesters than with benzoyl CoA. For short-hydrocarbon-chain (C_3 and C_4) thioesters (entries 10A, 11A, and 12A) the efficiencies were 1.7, 12, and 19 times greater, respectively, than with benzoyl CoA, with the branched C_4 isobutyryl CoA (entry 23A) as the exception, being 4 times slower. Compared to the specificity constant of *m*TBT for benzoyl CoA, other alkanoyl CoA's (acetyl and hexanoyl, entries 9A and 22A) were utilized by the mutant benzoyltransferase at lower specificities (0.49 and 0.24 min^{-1} mM^{-1}, respectively); cyclohexanoyl CoA was also utilized by *m*TBT to form a 2-*O*-acyl-2-*O*-debenzoyl analogue, but the reaction was orders of magnitude slower. The efficiency of *m*TBT with heterocarbonyl thioesters 3-furanyl- and 2- and 3-thiophene-carbonyls (Table 1, entries 17A, 18A, and 19A) were 1.2, 1.6, and 1.6 times greater, respectively, than with benzoyl CoA, while 2-furanyl- and 5-thiazole-carbonyls were 2.0 and 5.1 times less efficient than the natural substrate (entries 16A and 20A, respectively).

K_M and k_{cat} Values of *m*TBT with 7,13-*O*,*O*-Diacetyl-2-*O*-debenzoylbaccatin III and Various Aroyl CoA's. Still guided by efforts to conserve the stocks of the synthetically acquired acyl CoA's and the semisynthetic 2-*O*-debenzoyl taxane substrate, k_{cat} values were separately calculated at apparent saturation (1 mM) for the taxane substrate and each of the 19 productive aroyl CoA's at apparent saturation (estimated at 1 mM) for 5 min, in triplicate runs. Each sample was analyzed by LC-ESIMS/MS to verify the identity of the 2-*O*-acylated product and to quantify the relative rate at which the biosynthesized products were formed. The K_M values were calculated by multiplying the k_{cat} values by the reciprocal of the corresponding catalytic efficiency values (K_M/k_{cat}) (Table 1). For *m*TBT assays with 3-methylbenzoyl- and cyclohexanoyl-CoA, the turnover of substrate to product was comparatively 70- and 700-fold slower, respectively, than the other CoA thioesters used. In the assays conducted earlier, the relative k_{cat}/K_M values for these substrates could not be calculated since they were not strong competitive inhibitors of benzoyl CoA at 50 μM incubated for 5 min in the mixed substrate assays; within this period, their derived taxane products could not be detected, even at 1 mM. The rates at which the product was formed from 3-methylbenzoyl- and cyclohexanoyl-CoA by *m*TBT catalysis were therefore considered first-order (i.e., significantly below enzyme saturation, i.e., k_{cat}) at 1 mM after incubating for 4 h and are reported as v_o (cf. Table 1, entries 3B and 24B). The other CoA substrates (entries 2, 8, 13, 14, and 21, Table 1) were incubated similarly at 1 mM for 4 h, and the corresponding biosynthetic products derived by *m*TBT catalysis were not detectable.

*m*TBT showed similar to superior catalytic efficiency with several acyl coenzyme A thioesters (Table 1, entries 4, 5, 10−12, and 17−19, in column A) compared to benzoyl CoA. Calculating the k_{cat} values of *m*TBT for various acyl CoA's, however, revealed which kinetic parameter (k_{cat} or K_M) most influenced the magnitude of the efficiency parameter. Butenoyl CoA (Table 1, entry 12) was ~19-fold more efficient with *m*TBT than was benzoyl CoA. This difference was predominantly dictated by the near 9-fold greater turnover of butenoyl CoA over benzoyl CoA by *m*TBT, coupled with the ~2-fold decrease in K_M for butenoyl CoA over the natural CoA substrate. Conversely, the magnitude of the catalytic efficiency of *m*TBT for 3-furanoyl CoA (entry 17A, 2.2 min^{-1} mM^{-1}), which was nearly equal to the efficiency of *m*TBT for benzoyl CoA (1.8 min^{-1} mM^{-1}), was predominantly influenced by K_M. While the turnover number (k_{cat}) for the 3-furanoyl donor was 14-fold slower, the K_M was 17-fold lower (6.4 μM) for this substrate compared to that calculated for benzoyl CoA (110 μM), indicating that the catalytic efficiency was balanced by superior binding of the former acyl CoA. Compared to the K_M for benzoyl CoA, *m*TBT displayed lower K_M values for eight aroyl CoA substrates (Table 1, entries 4, 11, 12, 15, 17, 18, 22, and 23; column C). There are only three instances (entries 4, 17, and 18), however, where a lower K_M offset the deficient turnover rate that reciprocally equalized (or increased) the magnitude of the specificity constant (entries 4A, 17A, and 18A) of *m*TBT compared to that for benzoyl CoA.

The results of this study demonstrated the expansive substrate specificity of the recombinantly expressed mutant of the wtTBT (*m*TBT) in purified form when incubated with several acyl-CoA donor substrates and 7,13-*O*,*O*-diacetyl-2-*O*-debenzoylbaccatin III. *m*TBT transferred aroyl 4-substituted benzoyl analogues and 2- and 3-heterole carbonyl groups, including 5-thiazole carbonyl, which is a similar structural motif found in the antimitotic epothilone drug family.[24] A benefit of chemoselective biocatalytic attachment of heterole carbonyls onto the taxane core is that the diene functional group can potentially be further modified, for example, by Diels−Alder chemistry to form novel heterocyclic taxanes with biological activity. Notably, a previous investigation showed that the *Taxus N*-benzoyltransferase on the paclitaxel biosynthetic pathway indiscriminately transferred *o*-, *p*-, or *m*-substituted benzoyl groups from CoA, with a slight bias for the *p*-isomer.[22] In contrast, *m*TBT showed singular preference for the *p*-substituted regioisomers within a homologous series and only marginally recognized 3-methylbenzoyl CoA as a substrate. Therefore, the positioning of the substituent on the aromatic ring of aroyl CoA substrates may reveal that occluding sterics are present in the active site of *m*TBT. It was hypothesized that *m*TBT, characterized as a benzoyltransferase, would transfer aroyl groups more efficiently to the 2-*O*-debenzoyl substrate; therefore, the superior catalytic constants of the catalyst for C_3 and C_4 hydrocarbonoyl CoA's and butenoyl CoA's were phenomenological. Short-chain alkanoyl and alkenoyl groups and a cyclohexanoyl group from the CoA donor to the diterpene co-substrate were also transferred to the taxane acceptor substrate by *m*TBT (cf. Table 1). Likely, the active site of *m*TBT can accommodate the conformational flexibility and smaller size of the acyclic CoA substrates, including the various conformations of the cyclohexanoyl moiety. The transfer of these latter groups by *m*TBT indicates that the aromatic ring of the acyl CoA is not obligatory for catalysis.

By understanding the scope of the *m*TBT specificity, the current biological sources of the antimitotic drug paclitaxel (cell cultures derived from *Taxus* spp.,[25] yeast,[26] and several fungal[27,28] cultures that biosynthesize paclitaxel) can potentially be utilized to produce novel paclitaxel molecules. To date, only acetyl, benzoyl, 2-methylbutenoyl, and 2-methylbutanoyl have been identified at the C-2 hydroxy group of naturally occurring taxanes.[29] The array of C-2-*O* adducts in vivo can be conceivably expanded by separately feeding one of the several carboxylic acids as a substrate to a paclitaxel-producing organism engineered to produce any of the acyl CoA thioesters (described herein) for the construction of an unnatural paclitaxel pathway intermediate modified at C-2 by *m*TBT catalysis.

As mentioned previously, TBT is included in a distinct phylogenetic clade containing other benzoyltransferases. The wide

specificity of *m*TBT includes several non-natural CoA substrates and thus supports the "patchwork model" of metabolic pathway evolution. This model hypothesizes that an organism uses minimal gene content to provide a biocatalyst with maximum biochemical flexibility to provide product diversity, a model envisioned for the survival of an ancestral organism.[30] The broad specificity of *m*TBT suggests that this catalyst has likely maintained the flexibility it possessed during the early stages of evolution, according to the patchwork model. The several different kinds of acyl groups transferred in assays containing *m*TBT in vitro are remarkable, especially considering the limited, naturally occurring acyl CoA thioester substrates [acetyl, benzoyl, 2-methylbutenoyl, and 2-methylbutanoyl, which are variable with regard to sterics and electronics] available in the native host. Obviously, the acyl groups attached to the various taxane acceptors in planta at the C-2 hydroxy group of naturally occurring taxanes are likely sufficient to confer the necessary fitness to the host. While it is reasonable to speculate that the specificity of *m*TBT was already honed by the few acyl CoA substrates based on metabolite occurrence, the latent extended specificity of the benzoyltransferase suggests a relatively tolerant active site of *m*TBT on the taxane biosynthetic pathways. Obviously, the range of alkanoyl, alkenoyl, and aroyl CoA thioesters accommodated by the catalyst in this study has been established over the course of evolution by the modest pool of dissimilar natural CoA substrates in the original hosts.

Other BAHD family acyltransferases[22,31,32] also display broad substrate specificity profiles with varying acyl CoA donors and a range of alcohol and amine acceptor substrates. The current knowledge base of the BAHD acyltransferases, however, does not provide sufficient mechanistic information that enables speculation on what moderates the kinetic parameters of *m*TBT in terms of substituent regiochemistry in the aroyl CoA substrate, regarding sterics and electronic effects, and preferential catalytic efficiency for acyclic hydrocarbon carbonyls. Foreseeably, as more structural information becomes available for these BAHD acyltransferases, valuable insight into the mechanism of substrate specificity can be dissected. Moreover, directed evolutionary analyses can be employed to potentially produce new catalyst derivatives that are able to transfer an even greater or more refined scope of novel acyl groups to the taxane core or other diterpene scaffolds.

Experimental Section

Substrates, Reagents, and General Instrumentation. Baccatin III and 10-deacetylbaccatin III were purchased from Natland (Research Triangle Park, NC). Sodium [^{3}H]borohydride was purchased from American Radiolabeled Chemicals Inc. (Saint Louis, MO). The restriction endonucleases were purchased from New England Biolabs (Ipswich, MA). Acyclic short-chain-hydrocarbon carbonyl CoA's and all other reagents were obtained from Sigma-Aldrich and used without further purification, unless indicated otherwise. A Varian Inova-300 or a Varian UnityPlus500 instrument was used to acquire ^{1}H NMR spectra.

Subcloning the Wild-Type TBT cDNA. Standard microbial and recombinant techniques used throughout this work were described by Sambrook.[33] Turbo *Pfu* DNA polymerase (Stratagene) was used in all the PCR reactions. A sticky-end PCR method[34] was conducted to amplify wild-type *tbt* from *Taxus cuspidata* (accession no. AF297618) with an appropriate primer set [pair 1: forward primer (5′-*TG*GGCAGGTTCAATGTAGAT-3′) and reverse primer (5′-*GATCC*TTATAACTTAGAGTTACATATTTTAGCCAC-3′); pair 2: forward primer (5′-*TATG*GGCAGGTTCAATGTAGAT-3′) and reverse primer (5′-*C*TTATAACTTAGAGTTACATATTTTAGCCAC-3′); the nucleotides of *Bam*HI and *Nde*I restriction sites are italicized and underlined]. By this method, the *T. cuspidata tbt* cDNA was transferred from the previously used pCWori+ vector[35] to pET28a (Novagen), designated p28wtTBT. This exchange incorporated an *N*-terminal His_6-tag epitope on the expressed TBT for immunoblot analysis of the expressed protein and purification by His-Select Nickel Affinity Gel (Sigma, St. Louis, MO) binding. The plasmid containing the *tbt* cDNA and a pET28a vector without an insert were used to separately transform *E. coli* BL21(DE3) following a described protocol (Stratagene).

Site-Directed Mutagenesis of wt-*tbt*. Two point-mutations were incorporated into the wild-type *tbt* cDNA, while ligated in the pET28a vector, using the QuikChange XL Site-Directed Mutagenesis Kit (Stratagene) to change codon 19 from CAA to CCA, and codon 23 from AAT to AAA, with the following oligonucleotide sets [forward primer (5′-CGCCATGCCTT*CCA*TCGCCCAAA*AAA*ATCC-3′) and reverse primer (5′-GGTGCAGGAT*TTT*TTTGGGCGA*TGG*AAGGC-3′); the nucleotide mutation sites are italicized and underlined]. The amino acid replacements Q19P and N23K were made by these mutations in the encoded protein sequence of the wt-*tbt*, respectively; the resultant plasmid was designated p28PK-TBT and used to transform *E. coli* BL21(DE3) cells.

Protein Expression and Assessing Relative Soluble Expression Levels. The wild-type *tbt* and the point mutant *tbt* were expressed in *E. coli*, and the respective recombinant enzymes were harvested according to the previously reported protocol with some modifications.[2] In brief, BL21(DE3) bacterial cultures transformed to express either the wild-type or the modified *tbt* clone were grown overnight at 37 °C in 5 mL of Luria−Bertani medium supplemented with 50 μg/mL kanamycin. The 5 mL inoculum was separately added to 1 L of Luria−Bertani medium supplemented with the appropriate antibiotic, the cells were grown at 37 °C to an $OD_{600} \approx 1$, gene expression was induced with 50 μM isopropyl-β-D-1-thiogalactopyranoside, and the cultures were incubated at 18 °C. After 16 h, the density of cultures was assessed by OD_{600} monitoring. The cells were harvested by centrifugation at 4 000*g* for 20 min at 4 °C and resuspended in assay buffer [25 mM 3-(*N*-morpholino)-2-hydroxypropanesulfonic acid, 5% glycerol (v/v), 3 mM dithiothreitol, pH 7.4] to a concentration of 0.3 g cells/mL. The cells were lysed by sonication at 4 °C [5 × 1 min bursts at 50% power with 1 min intervals, and then 2 × 15 s bursts at 70% power with 2 min intervals, using a Misonix XL-2020 sonicator (Farmingdale, NY)]. The homogenate was centrifuged at 15000*g* to pellet the debris; the supernatant was clarified by centrifugation at 190 000*g* to provide the soluble enzyme fraction. The relative concentration of recombinantly expressed wild-type and mutant enzymes, i.e., wtTBT or *m*TBT, in the crude soluble fraction was assessed. Equal volumes of soluble protein extract isolated from each preparation were subjected to SDS-PAGE, and the separated proteins were visualized by Coomassie blue staining. Kodak 1D Image Analysis Software (Version 3.6.3) was used to integrate the intensity of the staining of the overexpressed TBT enzyme bands (at ~50 kDa) on the gel. From this data, the relative levels of soluble expression of the wtTBT and *m*TBT, the approximate enzyme purity, and the protein concentration by comparison against BSA standards ranging from 2 to 10 mg/mL were assessed. The relative overexpression amounts were also verified by Western immunoblot analysis, according to a method based on the 1-Step TMB-Blotting Kit (Pierce, Rockford, IL) with the following antibodies: monoclonal anti-polyhistidine and anti-mouse IgG peroxidase conjugate (Sigma, St. Louis, MO).

Synthesis of 7,13-*O*,*O*-Diacetyl-2-*O*-debenzoylbaccatin III. 7,13-*O*,*O*-Diacetyl-2-*O*-debenzoylbaccatin III was prepared according to an established procedure.[6] To a stirred solution of 7,13-*O*,*O*-diacetylbaccatin III[6] (100 mg, 149 μmol) in dry THF (7 mL) at 0 °C under N_2 was added (dropwise) bis(2-methoxyethoxy)aluminum hydride (>65 wt % in toluene, 3 equiv). After stirring for 2.5 h at 0 °C, the reaction was quenched by dropwise addition of saturated NH_4Cl, and the mixture was stirred for 10 min, then warmed to room temperature and diluted with EtOAc (50 mL), followed by the addition of H_2O (10 mL). The aqueous phase was separated and extracted again with EtOAc (2 × 25 mL). The combined organic fractions were washed with brine and H_2O and then dried over anhydrous Na_2SO_4. The solvent was evaporated, and the crude product was purified by silica gel flash column chromatography (10:90 to 60:40 (v/v), linear gradient of EtOAc in hexanes) to yield pure 7,13-*O*,*O*-diacetyl-2-*O*-debenzoylbaccatin III (54.8 mg, 65% yield): ^{1}H NMR (300 MHz, $CDCl_3$) δ 1.01 (s, H-16), 1.19 (s, H-17), 1.73 (s, H-19), 1.80 (ddd, J = 2.1, 3.6, 12.5 Hz, H-6β), 1.87 (d, J = 1.5 Hz, H-18) 1.99 (s, C(O)CH_3 at C-10), 2.11 (s, C(O)CH_3 at C-7), 2.12 (s, C(O)CH_3 at C-13), 2.18 (s, C(O)CH_3 at C-4), 2.44 (br s, OH at C-2), 2.55 (ddd, J = 2.4, 7.2, 14.3 Hz, H-6α), 2.67 (d, J = 4.8, H-14), 3.55 (d, J = 6.6 Hz, H-3), 3.87 (dd, J = 6.3, 11.4 Hz, H-2), 4.58 (dd, J = 10.8, 21.0 Hz, H-20), 4.94 (d, J = 7.8 Hz, H-5),

5.22 (dd, J = 3.6, 8.7 Hz, H-7), 6.12 (t, J = 8.8 Hz, H-13), 6.16 (s, H-10); LC-ESIMS (positive ion mode) m/z 589.20 $[M + Na]^+$.

Synthesis of 7-*O*-Acetylbaccatin III. To a stirred solution of baccatin III (100 mg, 170 μmol) in dry THF (3 mL) at 23 °C under N_2 were added Ac_2O (5 equiv), 4-DMAP (5 equiv), and Et_3N (24 μL, 172 μmol). The reaction was monitored by TLC, and upon completion, the reaction was diluted with EtOAc (50 mL) and quenched with H_2O (10 mL). The mixture was stirred for 15 min, and the aqueous fraction was separated and extracted with EtOAc (2 × 25 mL). The combined organic fractions were washed with saturated $CuSO_4$, brine, 0.1 M HCl, and H_2O and dried over anhydrous Na_2SO_4. The organic solvent was evaporated, and the crude product was purified by silica gel flash column chromatography (40:60 to 60:40 (v/v), linear gradient of EtOAc in hexanes) to yield pure 7-*O*-acetylbaccatin III (104 mg, 97% yield): ^1H NMR (500 MHz, $CDCl_3$) δ 1.06 (s, H-16), 1.11 (s, H-17), 1.77 (s, H-19), 1.80 (m, H-6β), 2.01 (s, C(O)CH_3 at C-7), 2.08 (s, H-18), 2.15 (s, C(O)CH_3 at C-10), 2.26 (s, C(O)CH_3 at C-4), 2.59 (ddd, J = 2.5, 8.5, 14.2 Hz, H-6α), 3.98 (d, J = 6.5 Hz, H-3), 4.13 (d, J = 8.5 Hz, H-20α), 4.29 (d, J = 8.5 Hz, H-20β), 4.83 (br t, H-13), 4.95 (d, J = 8.5 Hz, H-5), 5.58 (dd, J = 3.5, 7.0 Hz, H-7), 5.60 (d, J = 3.5 Hz, H-2), 6.25 (s, H-10), 7.46−8.08 (aromatic protons) (cf. Scheme 1 for position of proton and the number of protons at a particular position); LC-ESIMS (positive ion mode), m/z 651.20 $[M + Na]^+$.

Synthesis of 7-*O*-Acetyl-13-oxobaccatin III. To a stirred solution of 7-*O*-acetylbaccatin III (80 mg, 127 μmol) in dry CH_2Cl_2 (10 mL) at 23 °C under N_2 was added activated MnO_2 powder (1 g). The reaction was monitored by TLC, and upon completion of the reaction, the mixture was filtered to remove excess MnO_2. The filtrate was diluted with EtOAc (15 mL) and quenched with H_2O (10 mL). The aqueous fraction was separated and extracted with EtOAc (2 × 25 mL). The combined organic fractions were washed with brine and H_2O and dried over anhydrous Na_2SO_4. The organic solvent was evaporated, and the crude product was purified by silica gel flash column chromatography (30:70 to 60:40 (v/v), linear gradient of EtOAc in hexanes) to yield pure 7-*O*-acetyl-13-oxobaccatin III (79 mg, 100% yield): ^1H NMR (500 MHz, $CDCl_3$) δ 1.18 (s, H-16), 1.19 (s, H-17), 1.74 (s, H-19), 1.78 (ddd, J = 1.5, 3.0, 12.5 Hz, H-6β), 2.01 (s, H-18), 2.09 (s, C(O)CH_3 at C-7), 2.17 (s, C(O)CH_3 at C-10), 2.19 (s, C(O)CH_3 at C-4), 2.58 (ddd, J = 7.5, 9.5, 14.5 Hz, H-6α), 2.64 (d, J = 19.5 Hz, H-14β), 2.92 (d, J = 19.5 Hz, H-14α), 4.00 (d, J = 6.5 Hz, H-3), 4.08 (d, J = 7.0 Hz, H-20α), 4.30 (d, J = 8.5 Hz, H-20β), 4.90 (d, J = 8.5 Hz, H-5), 5.56 (dd, J = 7.5, 10.5 Hz, H-7), 5.63 (d, J = 7.0 Hz, H-2), 6.33 (s, H-10), 7.46−8.03 (aromatic protons) (cf. Scheme 1 for position of proton and the number of protons at a particular position); LC-ESIMS (positive ion mode), m/z 644.06 $[M + NH_4]^+$.

Synthesis of [13-^{3}H]-7-*O*-Acetylbaccatin III. To a stirred solution of 7-*O*-acetyl-13-oxobaccatin III (7 mg, 11 μmol) in dry THF (5 mL) at 0 °C under N_2 were added sodium [^{3}H]borohydride (333 μmol, specific activity of 150 Ci/mol) dissolved in a minimum amount of 0.01 M NaOH. The reaction mixture was warmed to room temperature, and the progress of the reaction was monitored by TLC. After 3 h, more 7-*O*-acetyl-13-oxobaccatin III (14.0 mg, 22 μmol) was added to the reaction, which was stirred for 3 h, diluted with EtOAc (5 mL), and quenched with H_2O (5 mL). The mixture was stirred for 15 min, and the aqueous fraction was separated and extracted with EtOAc (2 × 5 mL). The combined organic fractions were dried over anhydrous Na_2SO_4, the solution was filtered, the filtrate was concentrated in vacuo, and the crude product was purified on silica gel PTLC (60:40 (v/v), EtOAc/hexanes) to yield pure [13-^{3}H]-7-*O*-acetylbaccatin III (20 mg, 0.61 mCi, 95% radiochemical purity by radio-HPLC).

Synthesis of [13-^{3}H]-7,13-*O*,*O*-Diacetylbaccatin III. To a stirred solution of [13-^{3}H]-7-*O*-acetylbaccatin III (20 mg, 0.61 mCi) in dry THF (5 mL) at 23 °C under N_2 were added Ac_2O (100 equiv), 4-DMAP (40 equiv), and Et_3N (24 μL, 172 μmol), and the starting material was depleted after 28 h, as determined by TLC monitoring of the reaction progress. An aliquot of unlabeled 7-*O*-acetylbaccatin III (12 mg, 19 μmol) was added to the reaction and stirred in the solution for 3 h. The mixture was then diluted with EtOAc (5 mL), quenched with H_2O (5 mL), and stirred for 15 min; the aqueous fraction was separated and extracted with EtOAc (2 × 5 mL). The combined organic fractions were washed with saturated $CuSO_4$, brine, 0.1 M HCl, and H_2O and dried over anhydrous Na_2SO_4. The organic solvent was evaporated, and the crude product was purified on silica gel PTLC (60:40 (v/v), EtOAc/hexanes) to yield pure [13-^{3}H]-7,13-*O*,*O*-diacetylbaccatin III (21 mg, 0.59 mCi, 97% radiochemical purity by radio-HPLC).

Synthesis of [13-^{3}H]-7,13-*O*,*O*-Diacetyl-2-*O*-debenzoylbaccatin III. To a stirred solution of [13-^{3}H]-7,13-*O*,*O*-diacetylbaccatin III (21 mg, 0.59 mCi, 30 Ci/mol) in dry THF (5 mL) at 0 °C under N_2 was added (dropwise) bis(2-methoxyethoxy)aluminum hydride (Red-Al) (>65 wt % in toluene, 3 equiv). After stirring for 2.5 h, the reaction was quenched by dropwise addition of saturated NH_4Cl at 0 °C, and the mixture was stirred for 10 min, warmed to room temperature, and diluted with EtOAc (5 mL) and H_2O (5 mL). The aqueous phase was separated and extracted again with EtOAc (2 × 5 mL). The combined organic fractions were washed with brine and H_2O and then dried over anhydrous Na_2SO_4. The solvent was evaporated, and the crude product was purified by silica gel PTLC (60:40 (v/v), EtOAc/hexanes) to yield pure [13-^{3}H]-7,13-*O*,*O*-diacetyl-2-*O*-debenzoylbaccatin III (6.6 mg, 0.35 mCi, 99% radiochemical purity by radio-HPLC, 30 Ci/mol specific activity). The LC-ESIMS (positive ion mode) fragmentation profile and the ^1H NMR spectrum of authentic unlabeled 7,13-*O*,*O*-diacetyl-2-*O*-debenzoylbaccatin III, obtained as described,[6] were identical to those obtained for the [^{3}H]-labeled material.

Synthesis of Aroyl/alkyl CoA Thioesters. Several aroyl CoA donors (heteroaroyls and variously substituted benzoyls) were synthesized via a previously described method that proceeds through a mixed ethyl carbonate anhydride.[5] Briefly, Et_3N (3.0 μL, 30 μmol) was added to a solution of the a carboxylic acid (27 μmol) in 5:2 CH_2Cl_2/THF (v/v, 1.4 mL) under N_2 gas. The mixture was stirred for 10 min at 23 °C, ethyl chloroformate (2.9 μL, 30 μmol) was added in one portion, and the reaction was stirred for 1 h at 23 °C. The solvents were evaporated under reduced pressure, and the residue was dissolved in 0.5 mL of *t*-BuOH. Coenzyme A as the sodium salt (23 mg, 30 μmol dissolved in 0.5 mL of 0.4 M $NaHCO_3$) was added to the solution, and the mixture was stirred for 0.5 h at 23 °C and then quenched with dropwise addition of 1 M HCl, to adjust the pH to 3−5. The solvents were evaporated under vacuum, and the residue was dissolved in H_2O (5 mL, pH 5) and loaded onto a C18 silica gel column (10% capped with TMS) that was washed with 100% MeOH (50 mL) and pre-equilibrated with distilled H_2O (100 mL, pH 5). The sample was washed with H_2O (100 mL, pH 5) and then eluted with 15% MeOH in H_2O (50 mL, pH 5). The fractions containing aroyl CoA, as determined by TLC, were combined, and the solvent was evaporated to yield pure product (95−99% yield; data reported elsewhere[22]). The syntheses of cyclohexanoyl CoA and phenylacetyl CoA have not been previously reported, and their ^1H NMR data are included in the Supporting Information.

TBT Activity Assay and Protein Purification. An assessment of the relative quantity of solubly expressed wtTBT and *m*TBT in *E. coli* (described above) revealed that the recombinant *m*TBT enzyme partitioned into the soluble enzyme fraction approximately 5-fold better than the wild-type form. Therefore, an aliquot (0.9 mL) of the soluble *m*TBT preparation as a crude mixture, described in the previous section, was separately incubated at 31 °C with [13-^{3}H]-7,13-*O*,*O*-diacetyl-2-*O*-debenzoylbaccatin III (33 μM, 1 μCi) and 1 mM benzoyl CoA, and the total volume was adjusted to 1 mL with assay buffer. After 4 h, the reaction was quenched and extracted with EtOAc (4 × 2 mL), the respective organic fractions were combined, the solvent was evaporated, and the residue was dissolved in 50 μL of MeCN. A 25 μL aliquot was loaded onto a reversed-phase column (Econosphere C18, 5 μm, 250 × 4.6 mm, Alltech, Mentor, OH) and eluted at 1 mL/min with a linear gradient of solvent A:solvent B [solvent A: 97.99% H_2O with 2% MeCN and 0.01% H_3PO_4 (v/v); solvent B: 99.99% MeCN with 0.01% H_3PO_4 (v/v)] from 70:30 (v/v) to 40:60 (v/v) over 31 min, then to 0:100 (v/v) over another 2 min, and returning to the initial conditions over 7 min with a 5 min hold on an Agilent 1100 HPLC system (Agilent Technologies, Wilmington, DE). The HPLC was connected in series with a UV detector and a Packard Radiomatic Flow-One Beta 150TR radioactivity detector (Perkin-Elmer, Shelton, CT), which mixed the effluent with 3a70B Complete Counting Cocktail (Research Products International, Mount Prospect, IL). The UV absorbance and radioactivity profiles of the biosynthetic product isolated from the assays containing crude enzyme extracts of cells expressing *tbt* mutant were compared to those of the control assays containing extracts of cells transformed with vector without an insert.

Once active *m*TBT was verified by radiochemically guided assays, plasmid p28PK-TBT encoding the mutant *tbt* was expressed in large-scale (4 L), transformed *E. coli* cell cultures. After 16 h, the cells were harvested and processed as before except that, instead of 3-(*N*-morpholino)-2-hydroxypropanesulfonic acid buffer, the cell pellet was resuspended in 50 mM Na_3PO_4 buffer (pH 8.0), which was compatible

with the affinity resin used in a later purification step. The soluble fraction of each sample was separately loaded onto a Whatman DE-52 anion-exchange column (2.5 × 6 cm, 15 g resin) to remove small molecules and cell debris. A small fraction (~15%) of the total *m*TBT protein eluted in the flow-through and the remainder eluted from the ion-exchange resin in 100 mM NaCl (200 mL). The fractions containing *m*TBT enzyme were combined, and additional NaCl was added to a final concentration of 300 mM and incubated with His-Select Nickel Affinity Gel (3 g, Sigma-Aldrich) in batch mode at 4 °C. After 1 h, the mixture was poured into an Econo column (Bio-Rad, 20 cm × 2.5 cm), and the lysis buffer was drained. The resin was washed with seven column volumes of wash buffer (50 mM Na_3PO_4, 300 mM NaCl, 10 mM imidazole, pH 8.0), and the bound protein was eluted with a step-gradient of one column volume of elution buffer (50 mM Na_3PO_4, 300 mM sodium chloride, pH 8.0) containing 100 mM imidazole, followed by one column volume of elution buffer containing 200 mM imidazole. The imidazole was removed from the purified protein solution by consecutive concentration by ultracentrifugation (30 000 MWCO, YM30 membrane, Millipore, Billerica, MA) and dilution in assay buffer (25 mM 3-(*N*-morpholino)-2-hydroxypropanesulfonic acid, 5% glycerol (v/v), 3 mM dithiothreitol, pH 7.4). The recombinant protein migrated to an R_f by SDS-PAGE similar to that of the calculated molecular weight of TBT (~50 kDa), which was visualized by Coomassie blue staining. Kodak ID Image Analysis Software (version 3.6.3) was used to integrate the relative intensity of each type of enzyme band against BSA standards ranging from 2 to 10 mg/mL. The cells transformed with the vector without any insert were processed and purified similarly, and by comparison, TBT was not detectable by any of the detection methods described above.

Kinetic Evaluation of *m*TBT with 7,13-*O*,*O*-Diacetyl-2-*O*-debenzoylbaccatin III and Benzoyl CoA. Linearity of the rate of the *m*TBT-catalyzed reaction with respect to protein concentration and time was established with the natural benzoyl CoA at 50 μM, while the co-substrate 7,13-*O*,*O*-diacetyl-2-*O*-debenzoylbaccatin III was maintained at apparent saturation (1 mM) in 10 mL of assay buffer. Aliquots (1 mL) were collected, and the biosynthetic reaction was stopped by the addition of 500 μL of EtOAc at 5, 10, 20, 30, and 40 min and at 1, 2, 3, 4, and 5 h. Baccatin III (5 μg) was added as the internal standard to correct for the loss of analyte during the extraction of product with organic solvent. Each sample was extracted with EtOAc (2 × 4 mL), and the organic fractions were combined and then evaporated in vacuo. The resultant residue was dissolved in 200 μL of MeCN, and a 10 μL aliquot of the sample was loaded onto a reversed-phase column (Betasil C18, 5 μm, 150 × 2.1 mm, Thermo Fisher Scientific Inc., Waltham, MA), eluting at 0.3 mL/min with a linear gradient of solvent A:solvent B [solvent A: 99.50% H_2O with 0.5% H_3PO_4 (v/v); solvent B: 99.50% MeCN with 0.5% H_3PO_4 (v/v)] from 70:30 (v/v) to 0:100 (v/v) over 7 min, holding at 100% solvent B for 2 min, and returning to the initial conditions over 1.10 min, with a 50 s hold on a capillary HPLC system (CapLC capillary HPLC, Waters, Milford, MA). The effluent from the HPLC column was directed to an ESIMS/MS (Q-ToF Ultima Global, Waters, Milford, MA). The peak areas of the selected molecular ions $[M + H]^+$ and $[M + Na]^+$ derived by electrospray ionization of the biosynthetic product that was directed to and detected by the first-stage mass spectrometer were converted to concentration by comparison to the peak areas of the $[M + H]^+$ and $[M + Na]^+$ ions generated by authentic 7,13-*O*,*O*-diacetylbaccatin III ranging from 0 to 5 μM at 1.2 μM intervals. Samples containing high concentrations of biosynthetic product in the assays were diluted 10- to 20-fold so that the peak areas fell within the linear range of the MS detector.

Evaluation of the steady-state parameters was determined by incubating 50 μg of purified *m*TBT protein in 1 mL assays for 5 min. The concentration of benzoyl CoA was independently varied from 0 to 1000 μM in separate assays, while the 7,13-*O*,*O*-diacetyl-2-*O*-debenzoylbaccatin III was maintained at apparent saturation (1 mM). The initial velocity (v_o) was plotted against the co-substrate concentration, and the equation of the best-fit nonlinear regression curve ($R^2 > 0.99$) was determined (Microsoft Excel 2003, Microsoft Corp., Redmond, WA) to calculate k_{cat} and K_M.

Kinetic Evaluation of *m*TBT with 7,13-*O*,*O*-Diacetyl-2-*O*-debenzoylbaccatin III and Competing CoA Substrates. To identify productive co-substrates in pilot assays, 100 μg of purified *m*TBT in 1 mL of buffer, [13-^{3}H]-7,13-*O*,*O*-diacetyl-2-*O*-debenzoylbaccatin III (33 μM, 1 μCi), and an acyl CoA at 1 mM were incubated in the same reaction flask. The assays were incubated for 4 h at 31 °C, quenched, and extracted with EtOAc (2 × 4 mL). The organic fractions were evaporated in vacuo, and the resultant residues were separately dissolved in 50 μL of MeCN, loaded onto a reversed-phase column (Econosphere C18, 5 μm, 250 × 4.6 mm, Alltech, Mentor, OH), and eluted at 1 mL/min with a linear gradient of solvent A:solvent B [solvent A: 97.99% H_2O with 2% MeCN and 0.01% H_3PO_4 (v/v); solvent B: 99.99% MeCN with 0.01% H_3PO_4 (v/v)] on an Agilent 1100 HPLC system equipped for UV detection and radioactivity monitoring of the effluent. To confirm the identity of the products obtained from productive co-substrates, 100 μg of purified *m*TBT in 1 mL of assay buffer, 7,13-*O*,*O*-diacetyl-2-*O*-debenzoylbaccatin III, and an acyl CoA, each at 1 mM, were incubated in a mixture. After 4 h at 31 °C, the assays were quenched and extracted with EtOAc (2 × 4 mL). The organic fractions were evaporated in vacuo, and the resultant residue was dissolved in 200 μL of MeCN. A 10 μL aliquot was subjected to electrospray ionization, and the molecular ions ($[M + H]^+$ and $[M + Na]^+$) of the de novo biosynthetic 7,13-*O*,*O*-diacetyl-2-*O*-acyl-2-*O*-debenzoylbaccatin III analyte were detected in single-stage and tandem-mass spectrometer modes. The relative abundances, detected by the mass spectrometer, of selected ions between the various biosynthetic 2-*O*-acyl-2-*O*-debenzoylated samples at the same concentrations were shown to be identical among the following exemplary authentic standards (see Supporting Information for synthesis). The abundance of $[M + H]^+$ and $[M + Na]^+$ ions generated by identical electrospray ionization of authentic 7,13-*O*,*O*-diacetylbaccatin III, 7,13-*O*,*O*-diacetyl-2-*O*-debenzoyl-2-*O*-(3-fluorobenzoyl)baccatin III, and 2,7,13-*O*,*O*,*O*-triacetyl-2-*O*-debenzoylbaccatin III was separately quantified over a range from 0 to 5 μM at 1.2 μM intervals and then compared. Control assays in which one co-substrate and/or enzyme was omitted were processed and analyzed identically to the methods described above.

After productive CoA substrates were identified, the relative catalytic efficiency of *m*TBT with each productive acyl CoA thioester substrate identified above was assessed (based on a previous procedure).[23] Each CoA thioester (50 μM) was separately incubated with 50 μM benzoyl CoA, purified *m*TBT (50 μg), and 1 mM 7,13-*O*,*O*-diacetyl-2-*O*-debenzoylbaccatin III in a 1 mL assay for 5 min at 31 °C. The assays were processed similarly to the method described earlier in this report, including the addition of baccatin III (5 μg) as the internal standard to correct for losses during the extraction. The relative amount of each biosynthetic product made in each assay was resolved by LC-ESIMS. Samples containing product at concentrations above the linear range of detection of the mass spectrometer were diluted 20-fold prior to analysis. The peak areas in the following diagnoses were corrected with respect to the area under the $[M + H]^+$ and $[M + Na]^+$ ion peaks of the baccatin III internal standard. The sum of the corrected areas under the $[M + H]^+$ and $[M + Na]^+$ ion peaks of each biosynthetic 7,13-*O*,*O*-diacetyl-2-*O*-acyl-2-*O*-debenzoylbaccatin III analogues was divided by the sum of the total area under the peaks of the same ions of the biosynthetically derived 7,13-*O*,*O*-diacetylbaccatin III present in the same mixed-substrate assay. To assess the relative specificity constants for *m*TBT and each acyl CoA, the acquired ratios were each multiplied by the specificity constant (k_{cat}/K_M) of *m*TBT calculated from the Michaelis−Menten plot when benzoyl CoA and 7,13-*O*,*O*-diacetyl-2-*O*-debenzoylbaccatin III were used as substrates earlier. Productive acyl CoA substrates of *m*TBT that did not produce detectable product when assayed at 50 μM for 5 min under standard reaction conditions were incubated instead at 250 μM in the competitive substrate assays. In the latter case, the sum of the areas under the $[M + H]^+$ and $[M + Na]^+$ ion peaks of each 2-*O*-acylated biosynthetic product was reduced 5-fold and used as the numerator in the quotient, as described above, to calculate the relative k_{cat}/K_M of the less competitive CoA substrates.

Relative k_{cat} Values of *m*TBT with Various Acyl CoA Thioesters. The apparent maximal turnovers (k_{cat}) of *m*TBT for the productive acyl CoA thioesters, identified above, were assessed by incubating each CoA thioester (1 mM) separately with 50 μg of purified *m*TBT enzyme and 1 mM 7,13-*O*,*O*-diacetyl-2-*O*-debenzoylbaccatin III in a 1 mL assay for 5 min at 31 °C. The assays were extracted as described above, after the addition of baccatin III (5 μg) to each assay as the internal standard to correct for losses during extraction of the product. The amount of each biosynthetic product was determined by LC-ESIMS, as described previously. The sum of the peak areas of the $[M + H]^+$ and $[M + Na]^+$ ions of each *O*-acylated biosynthetic product (7,13-*O*,*O*-diacetyl-2-*O*-acyl-2-*O*-debenzoylbaccatin III) was converted to concentration by comparing the sum of the areas of the $[M + H]^+$ and

$[M + Na]^+$ ions of the concentration standards comprised of 7,13-*O*,*O*-diacetylbaccatin III, and the apparent k_{cat} of *m*TBT at saturating concentrations of each acyl CoA and 7,13-*O*,*O*-diacetyl-2-*O*-debenzoylbaccatin III was reported.

Acknowledgment. The authors thank Farhiya Hajiabdi, East Lansing High School, East Lansing, MI (ACS Project SEED), Mr. Mark Ondari, and Dr. Brad Cox for their technical assistance. The work in this report was supported by the Michigan Agricultural Experiment Station (MICL02107) and the Michigan State University College of Natural Science. The authors thank the Washington State Research Foundation (Pullman, WA) for the *wt-tbt* cDNA and the Michigan State University Mass Spectrometry Facility.

Supporting Information Available: LC-ESIMS/MS data for each of the biosynthesized 7,13-*O*,*O*-diacetyl-2-*O*-acyl-2-*O*-debenzoylbaccatin III analogues derived by catalysis of *m*TBT and the corresponding authentic derivatives; an amino acid sequence alignment of TBT *Taxus* orthologues and acyltransferases on the paclitaxel biosynthetic pathway; ^{1}H NMR data for each of the synthesized aroyl CoA analogues; a description of the synthesis of authentic 7,13-*O*,*O*-diacetyl-2-*O*-debenzoyl-2-*O*-(3-fluorobenzoyl)baccatin III, 2,7,13-*O*,*O*,*O*-triacetyl-2-*O*-debenzoylbaccatin III, and 7,13-*O*,*O*-diacetyl-2-*O*-debenzoyl-2-*O*-(3-thiophenecarbonyl)baccatin III, as model compounds; linear regression analysis of a concentration series of the 7,13-*O*,*O*-diacetylbaccatin III calibration standard plotted against the total ion current of the $[M + H]^+$ plus $[M + Na]^+$ ions measured by LC-ESIMS. This material is available free of charge via the Internet at http://pubs.acs.org.

References and Notes

(1) D'Auria, J. C. *Curr. Opin. Plant Biol.* **2006**, *9*, 331–340.
(2) St-Pierre, B.; De Luca, V. *Recent Adv. Phytochem.* **2000**, *34*, 285–315.
(3) Stewart, C., Jr.; Kang, B.-C.; Liu, K.; Mazourek, M.; Moore, S. L.; Yoo, E. Y.; Kim, B.-D.; Paran, I.; Jahn, M. M. *Plant J.* **2005**, *42*, 675–688.
(4) Ondari, M. E.; Walker, K. D. *J. Am. Chem. Soc.* **2008**, *130*, 17187–17194.
(5) Loncaric, C.; Merriweather, E.; Walker, K. D. *Chem. Biol.* **2006**, *13*, 1–9.
(6) Walker, K.; Croteau, R. *Proc. Natl. Acad. Sci. U.S.A.* **2000**, *97*, 13591–13596.
(7) Muchmore, D. C.; McIntosh, L. P.; Russell, C. B.; Anderson, D. E.; Dahlquist, F. W. *Methods Enzymol.* **1989**, *177*, 44–73.
(8) Flick, K.; Ahuja, S.; Chene, A.; Bejarano, M.; Chen, Q. *Malar. J.* **2004**, *3*, 50.
(9) Nishihara, K.; Kanemori, M.; Kitagawa, M.; Yanagi, H.; Yura, T. *Appl. Environ. Microbiol.* **1998**, *64*, 1694–1699.
(10) Yang, Q.; Reinhard, K.; Schiltz, E.; Matern, U. *Plant Mol. Biol.* **1997**, *35*, 777–789.
(11) Lemercier, G.; Bakalara, N.; Santarelli, X. *J. Chromatogr. B* **2003**, *786*, 305–309.
(12) Trevino, S. R.; Scholtz, J. M.; Pace, C. N. *J. Pharm. Sci.* **2008**, *97*, 4155–4166.
(13) Ma, X.; Koepke, J.; Bayer, A.; Fritzsch, G.; Michel, H.; Stoeckigt, J. *Acta Crystallogr., Sect D: Biol. Crystallogr.* **2005**, *D61*, 694–696.
(14) Ma, X.; Koepke, J.; Panjikar, S.; Fritzsch, G.; Stockigt, J. *J. Biol. Chem.* **2005**, *280*, 13576–13583.
(15) Chang, C.-H.; Schindler, J. F.; Unkefer, C. J.; Vanderberg, L. A.; Brainard, J. R.; Terwilliger, T. C. *Biorg. Med. Chem.* **1999**, *7*, 2175–2181.
(16) Gräslund, S.; Nordlund, P.; Weigelt, J.; Hallberg, B. M.; Bray, J.; Gileadi, O.; Knapp, S.; Oppermann, U.; Arrowsmith, C.; Hui, R.; Ming, J.; dhe-Paganon, S.; Park, H. W.; Savchenko, A.; Yee, A.; Edwards, A.; Vincentelli, R.; Cambillau, C.; Kim, R.; Kim, S. H.; Rao, Z.; Shi, Y.; Terwilliger, T. C.; Kim, C. Y.; Hung, L. W.; Waldo, G. S.; Peleg, Y.; Albeck, S.; Unger, T.; Dym, O.; Prilusky, J.; Sussman, J. L.; Stevens, R. C.; Lesley, S. A.; Wilson, I. A.; Joachimiak, A.; Collart, F.; Dementieva, I.; Donnelly, M. I.; Eschenfeldt, W. H.; Kim, Y.; Stols, L.; Wu, R.; Zhou, M.; Burley, S. K.; Emtage, J. S.; Sauder, J. M.; Thompson, D.; Bain, K.; Luz, J.; Gheyi, T.; Zhang, F.; Atwell, S.; Almo, S. C.; Bonanno, J. B.; Fiser, A.; Swaminathan, S.; Studier, F. W.; Chance, M. R.; Sali, A.; Acton, T. B.; Xiao, R.; Zhao, L.; Ma, L. C.; Hunt, J. F.; Tong, L.; Cunningham, K.; Inouye, M.; Anderson, S.; Janjua, H.; Shastry, R.; Ho, C. K.; Wang, D.; Wang, H.; Jiang, M.; Montelione, G. T.; Stuart, D. I.; Owens, R. J.; Daenke, S.; Schütz, A.; Heinemann, U.; Yokoyama, S.; Büssow, K.; Gunsalus, K. C. *Nat. Methods* **2008**, *5*, 135–146.
(17) Balbach, J.; Schmid, F. X. In *Frontiers in Molecular Biology*; Pain, R., Stefan, J., Eds.; Oxford University Press: New York, 2000; Vol. 32, pp 212−249.
(18) Kingston, D. G. I. *Pharmacol. Ther.* **1991**, *52*, 1–34.
(19) Kingston, D. G. I. *J. Nat. Prod.* **2000**, *63*, 726–734.
(20) Kingston, D. G. I.; Jagtap, P. G.; Yuan, H.; Samala, L. In *Progress in the Chemistry of Organic Natural Products*; Herz, W., Falk, H., Kirby, G. W., Eds.; Springer-Verlag Wien: New York, 2002; Vol. 84, pp 53−225.
(21) Taylor, G. F.; Thornton, S. S.; Tallent, C. R.; Kepler, J. A. *J. Labelled Compd. Radiopharm.* **1993**, *33*, 501–15.
(22) Nevarez, D. M.; Mengistu, Y. A.; Nawarathne, I. N.; Walker, K. D. *J. Am. Chem. Soc.* **2009**, *131*, 5994–6002.
(23) Pi, N.; Leary, J. A. *J. Am. Soc. Mass. Spectrom.* **2004**, *15*, 233–243.
(24) Gupta, M. L., Jr.; Bode, C. J.; Georg, G. I.; Himes, R. H. *Proc. Nat. Acad. Sci. U.S.A.* **2003**, *100*, 6394–6397.
(25) Xiao, W.-H.; Cheng, J.-s.; Yuan, Y.-J. *J. Biotechnol.* **2009**, *139*, 222–228.
(26) Engels, B.; Dahm, P.; Jennewein, S. *Metab. Eng.* **2008**, *10*, 201–206.
(27) Li, Y.-C.; Tao, W.-Y.; Cheng, L. *Appl. Microbiol. Biotechnol.* **2009**, *83*, 233–239.
(28) Gangadevi, V.; Muthumary, J. *Biotechnol. Appl. Biochem.* **2009**, *052*, 9–15.
(29) Baloglu, E.; Kingston, D. G. I. *J. Nat. Prod.* **1999**, *62*, 1448–1472.
(30) Holliday, G. L.; Thornton, J. M.; Marquet, A.; Smith, A. G.; Rebeille, F.; Mendel, R.; Schubert, H. L.; Lawrence, A. D.; Warren, M. J. *Nat. Prod. Rep.* **2007**, *24*, 972–987.
(31) D'Auria, J. C.; Chen, F.; Pichersky, E. *Plant Physiol.* **2002**, *130*, 466–476.
(32) Beekwilder, J.; Alvarez-Huerta, M.; Neef, E.; Verstappen, F. W. A.; Bouwmeester, H. J.; Aharoni, A. *Plant Physiol.* **2004**, *135*, 1865–1878.
(33) Sambrook, J.; Russell, D. *Molecular Cloning: A Laboratory Manual*; Cold Spring Harbor Laboratory Press, 2001.
(34) Zeng, G. *BioTechniques* **1998**, *25*, 788.
(35) Walker, K.; Schoendorf, A.; Croteau, R. *Arch. Biochem. Biophys.* **2000**, *374*, 371–380.

NP900524D